

Measuring Ion-Pairing in Buffer Solutions with Microwave Microfluidics

Angela C. Stelson, Charles E. Little, Nathan D. Orloff, Christian J. Long, and James C. Booth

National Institute of Standards and Technology, Communications Technology Laboratory
James.booth@nist.gov

Abstract— Microwave microfluidics is an emergent technique for characterizing conductivity and permittivity of fluids and has wide-ranging applications in the materials science and biomedical fields. The electrical properties of fluids as a function of frequency can be leveraged to characterize interface effects such as electrical double layers (EDL), solvent-mediated ion interactions, and bound water molecules. However, extraction of quantitative electrical properties over a wide range of frequencies (100 kHz-67 GHz) is nontrivial, and calibrations are required. Here, we utilize a microfluidics device with incorporated coplanar waveguides to characterize buffer solutions *in situ* and non-destructively. With a two-step fitting procedure, we fit relaxations associated with the EDL, water molecules, and ion-pairing in solution. We compare the three-Debye relaxation (water loss, ion-pairing and EDL relaxations fit to a Cole-Cole/Debye (water loss Cole-Cole and EDL Debye relaxations) model which does not include the ion-pairing relaxation, and find improved goodness of fit. This technique is broadly applicable to ionic solutions, and provides critical information about solvated ions in biological systems.

Index Terms— Permittivity measurement, Microfluidics, Transmission line measurements, Coplanar waveguides, Circuit testing

I. INTRODUCTION

Broadband dielectric measurements of fluids have been used to detect the electrical properties of proteins, particles, and cells in solution.[1]–[3] Integration of microfluidics with on-chip microwave devices and calibration techniques enables quantitative measurements of nanoliter volumes of fluids for pharmaceutical, chemical and biotechnology applications. Advances in microwave metrology have enabled on-chip broadband dielectric measurements from DC to 110 GHz. Measuring a wide frequency range allows us to characterize charge-based phenomena in fluids including electrical double layers (EDL), ionic conductivity and molecular re-orientations.[4]

Here, we utilized coplanar waveguides (CPW) integrated into microfluidics devices to measure the broadband electrical properties of Tris-acetate-ethylenediaminetetraacetic acid buffer with magnesium (TAE-Mg²⁺), which is commonly used in biological systems. Characterizing the electrical properties of ionic solutions is critical to advancing understanding of the interactions of biological systems with ions in solution. The frequency range (100 kHz-67 GHz) covered by our devices and calibration protocol captures both the low-frequency regime where EDL effects are strong, and the high-frequency regime where the solvent properties dominate. We extracted the electrical properties of bulk fluid, the EDL, and a weak signal that we associated with ion-pairing in the buffer [5]. We compared the

goodness of fit for a function without an ion-pairing relaxation (Cole-Cole/Debye), and found that it improved the goodness of fit for the broadband fluid properties when the ion-pairing relaxation was included.

II. METHODS

A. Device Fabrication

The device fabrication for the microwave microfluidics devices is described in detail in Ref. [4]. Briefly, all CPW structures were designed with 50 μm -wide center conductors, 5 μm -wide gaps and 200 μm -wide ground planes. In addition to CPWs of different lengths, devices including series resistors, series capacitors and short-circuited reflects were fabricated on the reference chip (bare device) to perform multiline-TRL [6] and series resistor calibrations [7]. We designed devices with two-layer microfluidic channels (test chip) consisting of ~ 50 μm of SU-8 photoresist, covered with an upper channel layer (~ 50 μm) of patterned polydimethylsiloxane (PDMS) (see Fig. 1B). The SU-8 microfluidic channels were ~ 80 μm wide, and exposed lengths of CPW to directly to fluid (0.5, 0.85, 1.55, and 3.314 mm). The CPW gap width and SU-8 height were chosen so that the electromagnetic fields interact with fluids and SU-8, not the PDMS layer. An acrylic press bar screwed into an aluminum chuck clamped the PDMS block to the chip (see assembled chip in holder in Fig. 1A).

B. Microwave Measurements

We measured the CPWs with a vector network analyzer (VNA) on a microwave probe station (Fig. 1A-B). We measured the S-parameters at 640 frequency points from 100 kHz to 67 GHz on a logarithmic frequency scale, at an RF power of -20 dBm, and with an intermediate frequency (IF) bandwidth of 10 Hz. We performed our measurements on a temperature controlled stage programmed to $25^\circ\text{C} \pm 2^\circ\text{C}$. We performed a multiline thru-reflect-line (TRL) calibration to determine the propagation constant of the bare-CPW lines (γ_0), followed by the series-resistor calibration to compute the capacitance per unit length of the bare CPW section (C_0). For frequencies below 1 GHz, we use the series resistor calibration to determine C_0 , and average the extracted circuit parameters across five line lengths. The propagation constant for the bare CPW lines is:

$$\gamma_0 = \sqrt{(R_0 + i\omega L_0)(G_0 + i\omega C_0)}, \quad (1)$$

where ω is the angular frequency and R_0 , L_0 , G_0 , and C_0 are the

distributed resistance, inductance, conductance, and capacitance per unit length of the bare-CPW lines, respectively. Here we assume that the CPW waveguide mode is TEM and that there are no magnetic materials present. Under these conditions, R_0 and L_0 are not sensitive to the dielectric properties of the surrounding materials. We derived the propagation constant of a non-magnetic loaded line:

$$\gamma_{tot} = \sqrt{(R_0 + i\omega L_0)(G_{tot} + i\omega C_{tot})}, \quad (2)$$

where G_{tot} and C_{tot} are the distributed conductance and capacitance per unit length of the fluid-loaded CPW lines, respectively. Then we solved for the G_{tot} and C_{tot} by taking the square of the ratio (1) divided by (2) as,

$$G_{tot} + i\omega C_{tot} = \frac{\gamma_{tot}^2}{\gamma_0^2} \cdot i\omega C_0. \quad (3)$$

For our measurement devices (Fig. 1A), the conductivity of quartz is negligible, thus G_0 is approximately zero. In practice, we obtain G_{tot} and C_{tot} two different ways. For high frequencies (1-67 GHz), we used the microfluidic-multiline TRL calibration on the microfluidic test chip to obtain γ_{tot} and γ_0 . For lower frequency measurements (less than 1 GHz), we de-embedded our raw measurements to the fluid-loaded portion of the line by accounting for the effect of cables, probes, and the CPW sections leading up to the fluid. Next, we performed a nonlinear least squares optimization to extract the propagation constant of the fluid-loaded and bare CPW test structures.

C. Equivalent Circuit Model

We developed a circuit model to describe total admittance $Y_{tot} = G_{tot} + i\omega C_{tot}$ of the TAE-Mg²⁺ buffer (Fig. 1C):

$$\frac{1}{Y_{tot}} = \frac{2}{Y_{EDL}} + \frac{1}{Y_f}, \quad (3)$$

where Y_{EDL} and Y_f are the admittances of the EDL and fluid,

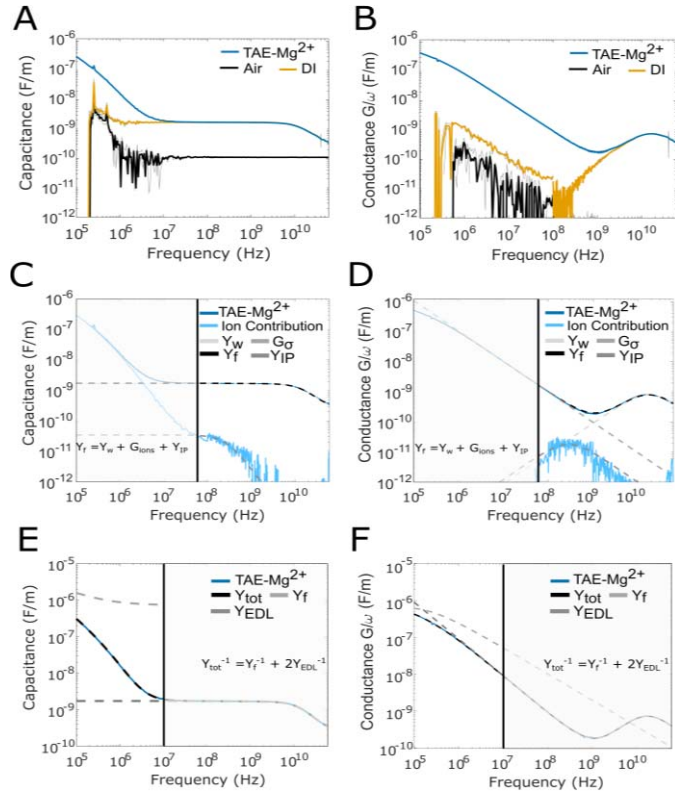


Fig. 2. (A) Broadband capacitance C and (B) conductance G per-unit-length of air, DI water and TAE-Mg²⁺ buffer. (C, D) Fitting procedure of high-frequency response of TAE-Mg²⁺ (dark blue solid line) with regions of fitting assigned for the water, ion and relaxations. Fit of (C) C_f and (D) G_f (black), fit of C_w and G_w (light gray), fit of C_{ions} and G_{ions} (medium gray), ion contribution (difference between data and $Y_w + G_\sigma$, light blue), and G_σ (gray in (D)). (E, F) Fit of C_{tot} and G_{tot} (black), fit of C_f and G_f (gray) and fit of C_{EDL} and G_{EDL} (light gray). Shaded regions indicate regions of data not included in the fitting step.

respectively. The fluid admittance, Y_f , is described as four parallel distributed circuit components (Fig. 1d):

$$Y_f = Y_{IP} + Y_w + G_\sigma + i\omega C_\infty \quad (4a)$$

$$Y_f = i\omega \frac{C_{IP}}{1+(i\omega\tau_{IP})} + i\omega \frac{C_w}{1+(i\omega\tau_w)^{1-\alpha_w}} + G_\sigma + i\omega C_\infty \quad (4b)$$

where C_∞ is the capacitance of the suspension far above the relaxation of water, C_w is the dipolar contribution of the water, G_σ is the conductance due to ions, and C_{IP} is the dipolar contribution of ions in the suspension. G_{IP} and G_w (Fig. 1D) represent the loss (imaginary part) of the Debye relaxations (Y_w and Y_{IP}) and are related to C_w and C_{IP} via the Kramers-Kronig relations. The time constants τ_w and τ_{IP} correspond to the rotational relaxation times of the water and the ion-counterion pair, respectively. We describe the EDL as operating in series with the admittance of the fluid for fluids with dissolved ions (Fig 1C). The EDL can be modelled as a Cole-Cole relaxation[4], where C_{EDL} is the capacitance associated with the EDL, α_{EDL} is a shape-broadening parameter and τ_{EDL} is the characteristic relaxation time associated with the formation of the EDL under electric field. The Cole-Cole relaxation is in parallel a constant phase element Y_{CPE} (Fig. 1E). [4] By developing an equivalent circuit

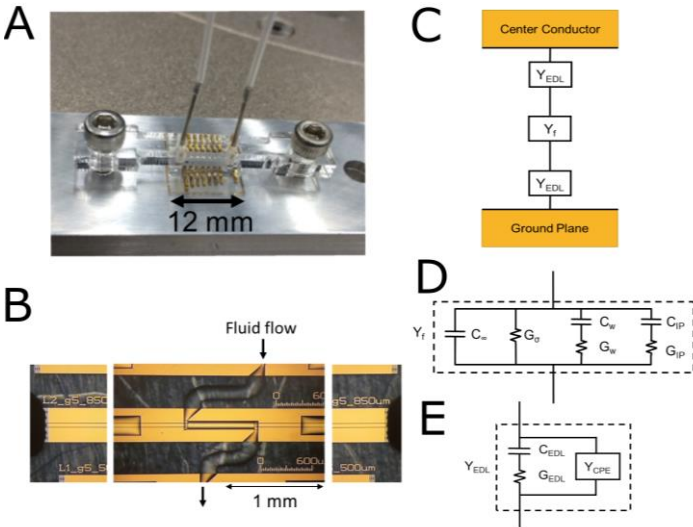


Fig. 1 Device design and measurement setup. (A) Image of microwave microfluidics device. (B) Composite microscope image of microfluidic channels with microwave probes landed. (C-E) Circuit model that describes the admittance of (C) the CPW, (D) fluid Y_f , and (E) the EDL Y_{EDL} .

model based on Debye-type relaxations, we can utilize broadband microwave measurements to extract physical parameters associated with these relaxations. Here we compare a three Debye model where $\alpha_w = 0$ with a Cole-Cole/Debye model, where $C_{IP} = 0$.

III. RESULTS

D. Broadband Microwave Measurements: C_{tot} and G_{tot}

The calibrated distributed conductance and capacitance for measurements of air, de-ionized water (DI water), and TAE-Mg²⁺ buffer is shown in Figs. 2a and 2b. To interpret the electromagnetic properties of the buffer over six decades of frequency, we assign regions of the frequency spectrum physical meaning for C_{tot} and G_{tot} . Below 10 MHz, there is a peak in the conductance and a drop in the capacitance in the buffer, which we attribute to the relaxation of the EDL. The capacitance contribution from the EDL was significant compared to the fluid, approximately two to three orders of magnitude larger than the capacitance of the DI-loaded CPW. The bulk ionic conductivity G_{tot}/ω (region of constant slope from 10 MHz-1 GHz) increases in ionic solutions much like behavior of the TAE-Mg²⁺ buffer. At approximately 20 GHz, the relaxation is due to the cooperative relaxation of water molecules.

E. Fitting Procedure for Y_{tot}

To fit each relaxation with a Debye model, we performed a two-step fitting process. First, we modeled the high-frequency data (70 MHz- 67 GHz) to extract the water and ion relaxations, as well as the bulk fluid conductance G_σ . From this, we constructed the fluid capacitance and conductance (where $Y_f = G_f + i\omega C_f$), pictured in Figs. 2C-D (black dotted line). This model is the sum of the water Debye relaxation, the ion-pairing Debye relaxation and conductance associated with the ions. We propagated the fit parameters of Y_f to lower frequencies (100 kHz-10 MHz) to fit the EDL region and extract Y_{EDL} (fit pictured in Figs. 2e-f). The fit of the suspension Y_{tot} agrees with the calibrated measured C_{tot} and G_{tot} from 100 kHz to 67 GHz. The relaxation of the EDL was also pictured (light gray dotted line). Because we propagated fit parameters from the high frequency regime to the EDL regime, the overall fit was sensitive to small relaxation peaks at intermediate frequencies, which perturbed the EDL fit.

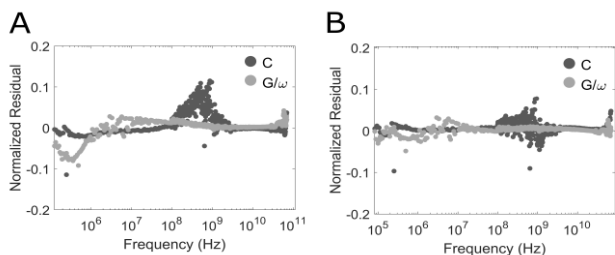


Fig. 3. Residuals of Y_{tot} fit normalized by the fit for (A) Cole-Cole/Debye fit of water with no ion-pairing for the high-frequency fit and (B) Three Debye fit with water, ion-pairing and EDL relaxations).

F. Goodness of Fit

Including the ion relaxation peak was necessary in TAE-Mg²⁺ buffer measurements to produce Debye-type relaxations for the EDL and resulted in overall lower residuals across the high frequency regime. Fig. 3 compares residuals for a Cole-Cole/Debye (Fig. 3A) model versus the three-Debye model (Fig. 3B). Including the ion-pairing relaxation results in smaller residuals more centered around zero along the full frequency spectrum. Systematic errors are smaller for the fit in both the high-frequency and the EDL regimes with the three-Debye model.

IV. CONCLUSION

In this report, we demonstrated broadband electrical measurements of TAE-Mg²⁺ buffer. We extracted physical parameters associated with dipolar relaxations in the fluid, and compared two models to fit the data (Cole-Cole/Debye and three-Debye). The three-Debye model has a better fit over the entire data range, demonstrating the necessity of including the ion-pairing relaxation. These broadband measurements can inform more sensitive narrowband measurements, which may be more cost-effective and lead to real-time assessment of biological systems.

ACKNOWLEDGMENT

This paper is an official contribution of NIST; not subject to copyright in the US. Usage of commercial products herein is for information only; it does not imply recommendation or endorsement by NIST.

REFERENCES

- [1] J. Leroy *et al.*, "Microfluidic biosensors for microwave dielectric spectroscopy," *Sensors Actuators, A Phys.*, vol. 229, pp. 172–181, 2015.
- [2] A. C. Sabuncu, J. Zhuang, J. F. Kolb, and A. Beskok, "Microfluidic impedance spectroscopy as a tool for quantitative biology and biotechnology," *Biomicrofluidics*, vol. 6, no. 3, 2012.
- [3] K. Grenier *et al.*, "Recent advances in microwave-based dielectric spectroscopy at the cellular level for cancer investigations," *IEEE Trans. Microw. Theory Tech.*, vol. 61, no. 5, pp. 2023–2030, 2013.
- [4] C. A. E. Little, N. D. Orloff, I. E. Hanemann, C. Long, V. M. Bright, and J. C. Booth, "Modeling Electrical Double-Layer Effects for Microfluidic Impedance Spectroscopy from 100 kHz to 110 GHz," *Lab Chip*, vol. 17, pp. 2674–2681, 2017.
- [5] A. Solutions *et al.*, "Is There an Anionic Hofmeister Effect on Water Dynamics? Dielectric Spectroscopy of," pp. 8675–8683, 2005.
- [6] R. B. Marks, "A Multiline Method of Network Analyzer Calibration," *IEEE Trans. Microw. Theory Tech.*, vol. 39, no. 7, pp. 1205–1215, 1991.
- [7] D. F. Williams and D. K. Walker, "Series-Resistor Calibration," in *50th ARFTG Conference Digest*, 1997, pp. 131–137.